A Computational Review of an Experimental Hint at Unusual Hydrogen Bonding in *o*-Cresol Cation Radical

Carl Trindle

Department of Chemistry, University of Virginia, Charlottesville, Virginia 22903

Received: October 11, 1999; In Final Form: February 28, 2000

We study the radical cations of *o*-cresol, which display interesting differential red shifts for the species in which the OH is inclined toward or away from the neighboring methyl group. We review four possible explanations: hydrogen bonding between OH and methyl, open shell effects, electrostatic environmental effects, and the perturbative admixture of antibonding σ MOs with the OH local bond orbital. The apparently analogous difference in the IR absorption of the OH stretch of *cis*- and *trans*-*o*-fluorophenol is easily rationalized by electrostatic effects. Methanol−methane radical cation shows a strong attractive interaction and has the linear X−HA arrangement and extended HA bond length characteristic of H-bonding. The cresol radical cation displays neither feature. Neither of these systems is a helpful analogy to *o*-cresol radical cation. The perturbative admixture of antibonding orbitals with the OH local MO provides an effective rationale for the *o*-cresol phenomena.

Introduction

In the course of their investigation of resonance-enhanced multiphoton ionization spectra of the S_1-S_0 transition of cresols, Fujii et al.[1] report the vibrational spectra of *o*-cresol cations. The neutral species display absorption arising from the OH stretch at 3655 cm^{-1} for both the cis and the trans orientations of the OH bond relative to the methyl substituent. The radical cations, however, show that the cis species absorbs at 3519 cm^{-1}, while the trans species absorbs at 3544 cm^{-1}. The meta cis and trans cation radicals differ in OH stretching absorption frequency by only about one wavenumber. The authors suggest that the modest red shift in the OH stretch may arise from an attractive interaction of OH with methyl, a kind of H-bonding. They draw an analogy with neutral fluorophenol, for which the cis and trans forms display differing OH stretching frequencies, with the cis form red-shifted relative to the trans form.

We investigated the structures and vibrational spectra of *cis*- and *trans*-*o*-cresol and associated cations by density functional theory and MP2 methods.[2]

We required first that the calculation be able to capture the phenomena. Our computed harmonic frequencies are collected in Table 1. As usual, the absorption frequencies are overestimated,[3] by 12% in (U)HF/6-31G*, by 3% in B3LYP/6-31G*, and by 5% in B3LYP using a better basis, i.e., 6-311+G**. The latter calculation, however, places the stretching frequencies for the neutral species closest together. Each computational model and basis correctly represents the greater red shift of the cis species attending ionization. There is also a fair consistency in the energetic values, shown in Table 2. The trans form is always favored energetically, but weakly.

Because we have shown that the experimental data are fairly well modeled by these computational methods, we will address two questions. Why is there *any* red shift? (The charge is removed only from the π manifold.) Given a red shift upon ionization, why is there a *different* red shift in cis and trans species?

TABLE 1: Frequencies and Shifts

system	exp	(U)HF (6-31G*)	MP2 (6-31G*)	B3LYP (6-31G*)	B3LYP (6-311+G**)
neutral cis	3655	4143	3774	3764	3841
neutral trans	3655	4121	3752	3751	3837
cis−trans shift	0	22	22	13	4
cation cis	3519	4010	3682	3656	3719
red shift cis	136	133	92	108	122
cation trans	3544	4002	3697	3660	3729
red shift trans	111	119	55	91	108
difference in red shifts	−25	−14	−37	−17	−14

TABLE 2: Absolute and Relative Energies

system	MP2 (6-31G*)	B3LYP (6-31G*)	B3LYP (6-311+G**)
neutral cis[a]	−345.6620516	−346.7826224	−346.8859412
neutral trans[a]	−345.6633068	−346.7835345	−346.8868286
ΔE trans−cis[b]	0.8	0.6	0.6
cation cis[a]	−345.3713263*	−346.4962161	346.5882527
cation trans[a]	−345.3735403	−346.4978994	−346.5900915
ΔE trans−cis[b]	1.4	1.1	1.2
IE cis[b]	182	180	187
IE trans[b]	182	179	186

[a] In hartrees. [b] In kcal/mol.

Discussion

Reasons for Any Red Shift. There are major structural changes attending ionization, as shown in Table 3A−C. We refer here to the MP2 results, but there is no noticeable difference between the quoted values and the DFT geometry. Structural changes include the following:

1. CO bond shortening, by about 0.04 Å;
2. COH angle opening from about 108° to about 112°;
3. ring distortion resulting from quinoid shortening of the C_3C_5 and C_1C_6 bonds; and
4. ring distortion at the substitution sites.

The OH distance does increase upon ionization, but by less than 0.01 Å. The cis−trans *difference* in OH extension is only 0.0011 Å. The local geometric changes are largely summed up

10.1021/jp993606m CCC: $19.00
Published on Web 05/11/2000

TABLE 3

A: Geometric Parameters (MP2/6-31G*)[a]

parameter (change upon ionization)[b,c]	values for cis		values for trans		values for phen	
	neutral	cation	neutral	cation	neutral	cation
OH distance	0.9737	0.9800	0.9737	0.9811		
C_2O distance (≪)	1.3766	1.3327	1.3777	1.3349	1.3752	1.3303
C_2C_3 distance (≫)	1.4045	1.4434	1.4040	1.4512	1.3971	1.4345
C_1C_2 distance (>)	1.3961	1.4159	1.3954	1.4011	1.3976	1.4096
C_1C_2-O valence angle	116.4	115.5	122.6	124.6	122.8	124.4
C_3C_2-O valence angle	122.4	122.1	116.1	113.9	116.8	114.1
C_2-OH valence angle (≫)	108.8	112.4	108.2	111.5	108.3	112.0
C_3C_5 distance (≪)	1.4000	1.3575	1.3970	1.3887	1.3968	1.3528
C_1C_6 distance (≪)	1.3931	1.3409	1.3967	1.3794	1.3933	1.3484

B: Geometric Parameters (B3LYP/6-311+G**)[a]

parameter (change upon ionization)[b,c]	values for cis		values for trans	
	neutral	cation	neutral	cation
OH distance	0.9621	0.9716	0.9626	0.9713
C_2O distance (≪)	1.3719	1.3115	1.3723	1.3138
C_2C_3 distance (≫)	1.4042	1.4505	1.4068	1.4561
C_1C_2 distance (>)	1.3943	1.4289	1.3964	1.4213
C_1C_2-O valence angle	116.8	115.7	122.2	122.5
C_3C_2-O valence angle	122.2	121.9	116.7	115.3
C_2-OH valence angle (≫)	110.1	113.6	108.1	113.4
C_3C_5 distance (<)	1.3978	1.3793	1.3968	1.3869
C_1C_6 distance (≪)	1.3906	1.3653	1.3961	1.3663

C: Geometric Parameters (B3LYP/6-31G*)[a]

parameter (change upon ionization)[b,c]	values for cis		values for trans	
	neutral	cation	neutral	cation
OH distance	0.9687	0.9780	0.9697	0.9780
C_2O distance (≪)	1.3709	1.3147	1.3723	1.3168
C_2C_3 distance, Me at C_3 (≫)	1.4071	1.4517	1.4068	1.4572
C_1C_2 distance (>)	1.3971	1.4315	1.3964	1.4239
C_1C_2-O valence angle	116.82	115.55	122.21	122.47
C_3C_2-O valence angle	122.20	121.97	116.68	115.20
C_2-OH valence angle (≫)	109.26	113.10	108.76	112.90
C_3C_5 distance (<)	1.3993	1.3814	1.3969	1.3892
C_1C_6 distance (≪)	1.3982	1.3690	1.3960	1.3698

[a] Distances are in Å, angles in degrees. [b] Change is coded as follows: ≪ means a marked decrease, < a lesser decrease, > an increase, ≫ a marked increase. [c] Numbering scheme for table 3A−C.

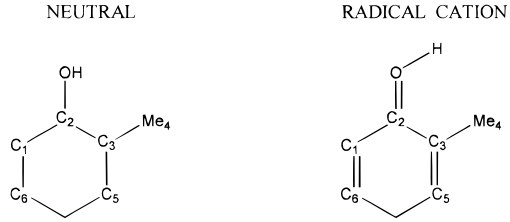

as a rehybridization at oxygen from sp^3 to sp^2 and the removal of an electron from one of the pseudodegenerate benzene π HOMOs.

Possible Explanations for a Differential Red Shift. In our discussion of the differential red shift, we will rely on the NBO analysis of Weinhold,[4] which we describe here. The NBO analysis resolves the electronic density of a molecular system into chemical entities that are familiar from Lewis structures, namely, cores, lone pairs, and pair bonds. These entities are assigned energies and occupation numbers that are typically close to the integers suggested by Lewis structures. The strictly local (one- or two-center) orbitals are resolved into LCAO components. Local antibonds are also defined and are also assigned (usually small) occupation numbers. These occupations arise from delocalization, a consequence in this analysis of the admixture of antibonding local orbitals with local bonding orbitals. Of great interest here is the perturbation analysis, which reports the extent of mixing of entirely local bonds with local antibonds, and the stabilization resulting from the admixture and attendant delocalization. Of course, the most important delocalization occurs in the π system; these effects are common to all such benzene-derived systems. The next most significant energy effects are associated with the mixing of σ antibonding local orbitals into σ bonding orbitals. One consistent and significant feature of this effect is that the admixture is most important when the bonding and antibonding orbitals achieve a trans orientation. σ CH and CC bonds are all subject to this kind of mixing, but we will pay closest attention to the OH bond and whatever antibonding orbitals are mixed into it. Typically, these are the antibonding σ orbitals associated with the CC bond in trans (antiperiplanar) disposition relative to the OH bond. Table 4 contains quantities selected from NBO reports on the B3LYP/6-311+G* calculations.

It is immediately striking that the NBO-assigned energies for the α and β components of the σ bonds in the cations are substantially different from the assigned energies of the corresponding σ bonds in the neutral species. Apparently, it is not justified to assume a direct correspondence between NBO bond energies and bond stretching frequencies. We might be surprised to see that the energies of the OH bonds in the neutral species differ noticeably (the cis, at −0.75017 hartrees, is 12.87 millihartrees more stable than the trans species' OH bond). However, the trans OH bond is more extensively stabilized in second order, compensating in part for this difference. This reminds us of the main shortcoming in the modeling, that, in the neutral *o*-cresols, the cis OH stretching frequency is slightly greater than the trans OH stretching frequency, although they are virtually identical according to experimental measurement. In the cations, the NBO-assigned energies of the OH bonds are much closer, differing only by 4.17 millihartrees (α) and 3.93 millihartrees (β). The trans bond is again more thoroughly stabilized in second order by the suitably oriented CC antibond. This CC bond is also longer, which helps us understand why this antibond is lower in energy and more thoroughly mixed into the OH bond. With due caution, we will use the NBO results in the following discussion of alternative explanations of the differential red shift in *o*-cresol cations.

Response A: H-Bonding. The small observed differential red shift might be attributed to OH−methyl attraction, a kind of H-bonding in the cis isomer that is absent in the trans isomer.

The methyl and hydroxyl substituents in *o*-cresol and its cations do not display the preferred collinear XH−Y geometry that is characteristic of familiar H-bonding species.[5] Nor do we observe any cis−trans differential in OH bond extension characteristic of H-bonding. No OH−methyl CH antibonding coupling is discernible in the NBO analysis in either the cis or the trans arrangement.

Methyl is not a typical participant in hydrogen bonding, but we find that there is a significant attraction between methyl and OH in the $[CH_4-H_2O]^{+\bullet}$ radical cation. The question presents itself, whether the $[CH_4-H_2O]^{+\bullet}$ radical cation is a helpful analogy to cresol. Our view is that the CH_4-H_2O interaction is

TABLE 4: NBO Values for the OH Bond in Cresols

species	charge	*N* (electronic occupation)	*E*(OH) (hartrees)	energy gap (hartrees)	mixing strength (hartrees)	second-order stablilization energy (kcal/mol)	total second-order stabilization energy (kcal/mol)
cis	cation	0.99323	−0.97011 α	1.26 α	0.66 α	2.18 α	4.37
		0.99325	−0.96448 *β*	1.26 *β*	0.66 *β*	2.19 *β*	
trans	cation	0.99340	−0.96594 α	1.22 α	0.67 α	2.29 α	4.56
		0.98906	−0.96055 *β*	1.23 *β*	0.67 *β*	2.27 *β*	
cis	neutral	1.98754	−0.75017	1.31	0.64	3.94	3.94
trans	neutral	1.98888	−0.73730	1.30	0.66	4.11	4.11

TABLE 5: Geometric Parameters for *o*-Fluorophenol (B3LYP/6-31G*)[a]

	values for cis		changes	values for trans	
parameter	B3LYP/6-31G*	B3LYP/6-311+G**	cis → trans	B3LYP/6-31G*	B3LYP 6-311+G**
OH distance	0.9720	0.9650	<0.01 Å	0.9697	0.9627
C_2O distance	1.3624	1.3617	<0.01 Å	1.3646	1.3632
C_2C_3 distance (F at C_3)	1.3979	1.3941	<0.01 Å	1.3979	1.4016
C_1C_2 distance	1.3955	1.3934	<0.01 Å	1.3946	1.3967
C_1C_2−O valence angle	119.95	120.49	opening 4°	123.99	124.19
C_3C_2−O valence angle	121.15	121.89	closing 4°	117.48	117.80
C_2−OH valence angle	107.26	109.16	opening <1°	108.58	109.52
C_3C_5 distance (<)	1.3835	1.3809	<0.01 Å	1.3854	1.3826
C_1C_6 distance (≪)	1.3963	1.3932	<0.01 Å	1.3977	1.3947

[a] Distances are in Å, angles in degrees.

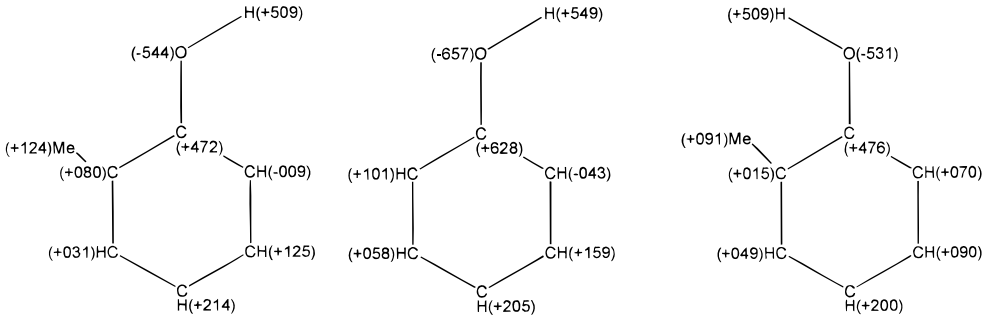

Figure 1. NBO charges in milli-electrons for *trans*-cresol RC (left), phenol RC (center), and *cis*-cresol RC (right). Parenthesized charges apply to the adjacent atoms or groups of atoms (e.g., CH) (see Discussion).

quite different from that in the *o*-cresol radical cation. First, the CH_4-H_2O system can arrange itself in the conventional linear O−H···C fashion. In the $[CH_4-H_2O]^+$ cation, the OH bond oriented toward the methane is substantially extended over that of its partner, as well as over either OH bond in the neutral CH_4-H_2O system. NBO analysis shows a substantial occupation of the OH antibond and some admixture with OH of the methane CH antibonds. No such admixture is to be found in the cresol radical cations. The analogy is inadequate, probably because the positive charge in the cresol systems is in the π manifold; that is not the case in the CH_4-H_2O system, where the positive charge is on the water fragment. We take the view that the extension of the idea of H-bonding to the cresol radical cation should be endorsed only if other explanations are unable to account for the data.

Response B: Electrostatic Environment. The small observed differential red shift might be attributed to differing electrostatic environments of cis and trans σ_{OH} bonds.

The OH induces an asymmetry in the ring in the phenol radical cation, in geometry and in charge distribution. The methyl substituent exaggerates the asymmetry, as we show in Figure 1.

Phenol radical cation (RC) shows a striking geometric distortion, in which the CC bond trans to the OH bond is extended (Table 3C). The α-cis and -trans carbons bear net negative and positive charges, respectively. In contrast, for cresol RC, the bond CC* in the chain OCC* (where C* is the methyl substitution site) is always lengthened, regardless of the orientation of the OH bond.

In cresol RCs, the charges at the α carbons depend on the orientation of the OH bond. The trans species shows a negative charge at the cis α carbon, smaller than the analogous negative charge in phenol RC. The cis species has a positive charge at both α carbons. The OH motion in phenol and *trans*-cresol RCs moves the positive hydrogen into a region of weakly negative (attractive) potential. The OH motion for *cis*-cresol moves the positive hydrogen into a region of positive (repulsive) potential. One would surmise that the OH frequency would be shifted more toward the blue for *cis*-cresol RC than for *trans*-cresol RC, contrary to experimental reports.

The electrostatic explanation *does* seem to describe the red shift of the OH stretch in neutral *cis*- versus *trans*-*o*-fluorophenol.[6] The frequencies for the OH stretch are 3634 cm^{-1} (cis) and 3662 cm^{-1} (trans), to be compared with that in phenol itself, 3658 cm^{-1}. The shift of 28 cm^{-1} is captured well by our DFT estimates. Using B3LYP/6-31G*, we find frequencies of 3726 and 3755 cm^{-1}, respectively, while using B3LYP/6-311+G**, we find 3809 and 3840 cm^{-1}, respectively. The shifts are thus 29 or 31 cm^{-1}. The structures of neutral *cis*- and *trans*-*o*-fluorophenol do not differ significantly, except in the CCO angles. (See Table 5.) NBO analysis of charges (Figure 2) shows that, in fluorophenol, the trans OH bond is destabilized and its stretch blue-shifted in the field of the parallel CH dipole, but the cis OH bond is stabilized and its stretch red-shifted in the

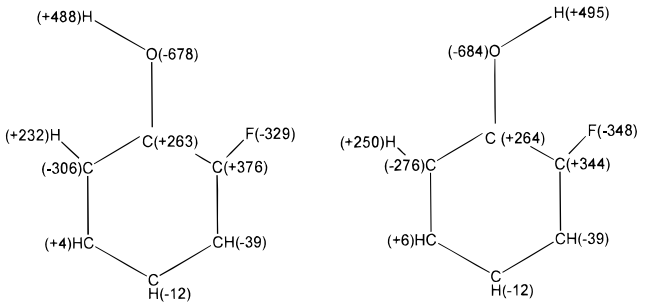

Figure 2. NBO charges in milli-electrons for *trans-o*-fluorophenol (left) and *cis-o*-fluorophenol (right). The trans OH bond is destabilized and blue-shifted in the field of the parallel CH dipole, but the cis OH bond is stabilized and red-shifted in the field of the antiparallel CF dipole.

field of the antiparallel CF dipole. (See Figure 2.) It would appear that this system is not a faithful analogy to the cresol radical cation. The fact that an electrostatic picture accounts for the difference in red shifts in this case cannot be taken as proof that the differential red shift in the *o*-cresols has an electrostatic origin.

Response C: Open Shell Effect. The small observed differential red shift might be attributed to differing σ_{OH^*} populations resulting from the presence of a RC's odd electron. An analogy might be drawn to the water−methane (or methanol−methane) RC.

As already noted, in the cresol RCs, the odd electron is largely confined to the π manifold. NBO analysis shows no significant occupation of the σ_{OH^*} orbital, in contrast to the behavior of the methane−water radical cation. Our MP2/6-31+G** description shows that the electron is removed from the water oxygen and that there is a strong association between the water radical cation and methane. Methane is "edge-protonated", and the OH bond involved is considerably lengthened. This account applies as well to the methane−methanol radical cation. The extension of the OH bond (0.995−1.045 Å in the smaller system) and the linear C···H−O arrangement are diagnostic of H-bonding. Neither geometric feature is displayed in the cresol radical cations. Any effect of the open shell is likely more indirect in cresol, through the changes in charge distribution and structure induced by the different π electron distribution.

Response D: Perturbative Mixture of σ_{OH} with Trans σ Antibonding σ_{CC^*}. The small observed differential red shift might be attributed to a differing σ_{CC^*} admixture and the attendant stabilization of the OH bond.

Discussion. NBO analysis (Table 4) shows that the major contaminant of the σ_{OH} local bond is the trans σ_{CC^*} local orbital. The extent of admixture depends on the energy of the σ_{CC^*} level. The longer CC bond has the more accessible empty antibonding level and is more effective in stabilizing the OH bond. Hence, the trans species, enjoying more effective perturbative stabilization, will have the stronger OH bond and the more blue-shifted OH stretch.

Conclusions

It is not necessary to imagine a new kind of hydrogen bonding to explain the differential red shifts in cis and trans conformations of the *o*-cresol radical cation. A convincing explanation lies outside the electrostatic picture thought to rationalize the geometric and energetic characteristics of hydrogen bonding. A preferable account takes a perturbation-theoretic view and attributes the differential red shift to a varying admixture of σ antibonding orbitals into the OH bond itself.

Acknowledgment. The author acknowledges financial assitance from the Department of Chemistry of the University of Virginia and the Body Foundation.

Supporting Information Available: Condensed output from Gaussian computations, NBO tables. This material is available free of charge via the Internet at http://pubs.acs.org.

References and Notes

(1) Fujii, A.; Fujimaki, E.; Ebata, T.; Mikami, N. A New Type of Intramolecular Hydrogen Bonding: Hydroxy-Methyl Interactions in the *o*-Cresol Cation. *J. Am. Chem. Soc.* **1998**, *120*, 13256.

(2) Frisch, M. J.; Trucks, G. W.; Schlegel, H. B.; Scuseria, G. E.; Robb, M. A.; Cheeseman, J. R.; Zakrzewski, V. G.; Montgomery, J. A., Jr.; Stratmann, R. E.; Burant, J. C.; Dapprich, S.; Millam, J. M.; Daniels, A. D.; Kudin, K. N.; Strain, M. C.; Farkas, O.; Tomasi, J.; Barone, V.; Cossi, M.; Cammi, R.; Mennucci, B.; Pomelli, C.; Adamo, C.; Clifford, S.; Ochterski, J.; Petersson, G. A.; Ayala, P. Y.; Cui, Q.; Morokuma, K.; Malick, D. K.; Rabuck, A. D.; Raghavachari, K.; Foresman, J. B.; Cioslowski, J.; Ortiz, J. V.; Baboul, A. G.; Stefanov, B. B.; Liu, G.; Liashenko, A.; Piskorz, P.; Komaromi, I.; Gomperts, R.; Martin, R. L.; Fox, D. J.; Keith, T.; Al-Laham, M. A.; Peng, C. Y.; Nanayakkara, A.; Gonzalez, C.; Challacombe, M.; Gill, P. M. W.; Johnson, B.; Chen, W.; Wong, M. W.; Andres, J. L.; Gonzalez, C.; Head-Gordon, M.; Replogle, E. S.; Pople, J. A. *Gaussian 98*, revision A.7; Gaussian, Inc.: Pittsburgh, PA, 1998.

(3) Scott, A. P.; Radom, L. *J. Phys. Chem.* **1996**, *100*, 16502.

(4) Glendening, E. D.; Badenhoop, J. K.; Reed, A. E.; Carpenter, J. E.; Weinhold, F. E. *NBO 4.0*; Theoretical Chemistry Institute, University of Wisconsin: Madison, WI, 1996.

(5) Levine, I. N. *Quantum Chemistry*, 5th ed.; Prentice Hall: New York, 2000; pp 705−707.

(6) Omi, T.; Shitomi, H.; Sekiya, N.; Takazawa, K.; Fujii, M. *Chem. Phys. Lett.* **1996**, *252*, 287.